Volume 4 JULY, 1933 Number 7

PHYSICS

A Journal of General and Applied Physics

A High Voltage Sensitivity Direct-Current Amplifier

P. A. MACDONALD AND E. M. CAMPBELL, *The Department of Physics, University of Manitoba*

(Received April 4, 1933)

It is shown that a negative resistance of a definite value, introduced into the plate circuit of a thermionic valve theoretically allows the voltage sensitivity to become infinite. Practical application is made to construct high sensitivity direct-current amplifiers. The data show a mutual conductance of 30,000 microamp. per volt.

THE analytical expression for the change in plate current resulting from a change of the potential impressed upon the control grid of a thermionic tube, connected in the manner of Fig. 1a, is

$$\partial i_p/\partial E_g = G_m/(1+R_p/Z_p), \qquad (1)$$

where i_p is the plate current, E_g the grid potential, G_m the mutual conductance of the tube, Z_p the filament-plate resistance of the tube and R_p the value of the resistance in the plate circuit.

If, as shown in Fig. 1b, the grid-filament system of a second thermionic tube be substituted in place of the ohmic resistance R_p, it will be possible to give R_p a negative value by adjusting the constants of the circuit in such a way that this second grid-filament system operates on the positive ion section of its grid potential *vs.* grid current curve.

If R_p is made negative and numerically equal to Z_p then the numerical value of the above algebraic expression becomes very great and a small change in the input potential E_g will cause a very great change in i_p, thus impressing a large voltage change on the second grid-filament system, G_2F_2. The introduction of the plate circuit of the second tube as in Fig. 3 will then result in a two tube amplifier of very high voltage sensitivity, the plate current of this tube being observed in relation to the grid potential of the first tube.

A circuit based on this principle has been recently discussed by Macdonald and Macpherson,[1] though at the time they did not attribute the high sensitivity to the negative sign of the resistance R_p, but to the change in the potential distribution of the circuit brought about by substituting the positive ion for the electron grid current of the output tube, a condition which we later found could not be brought about with the circuit as above described.

The properties of the circuit given in the previous communication and obtained by using a UX 222 as an input tube and a 112 A as the output tube are: (1) The plate current of the output tube may be controlled by the potential

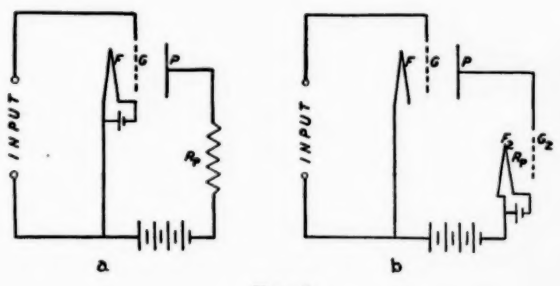

a b

FIG. 1.

[1] Macdonald and Macpherson, Phil. Mag. **15**, 72 (1933).

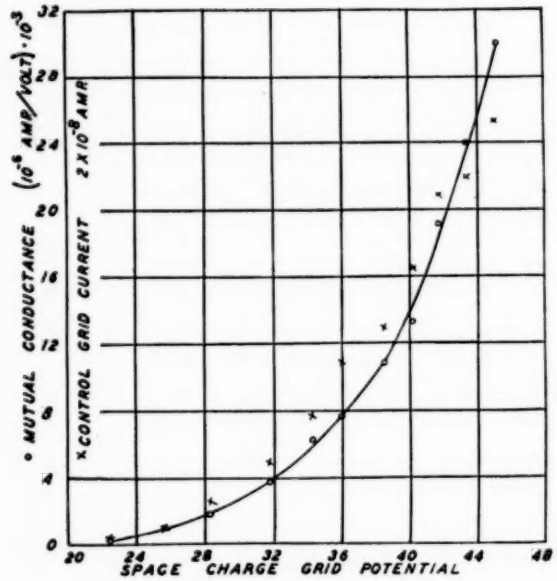

FIG. 2. The circles show how the mutual conductance of the amplifier increases with increasing space charge grid. The crosses are the values of the control grid current of a UX 222, measured at constant grid potential, for different values of the space charge. The similarity of the data shows how the grid resistance controls the voltage sensitivity.

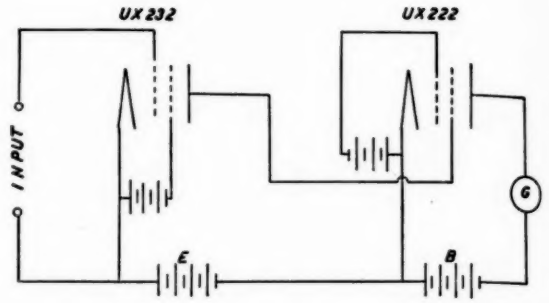

FIG. 3. Showing how two screen grid tubes may be connected to obtain a direct current amplifier of high sensitivity. The space charge grid in the output tube controls the voltage sensitivity.

of the control grid of the input tube. When the circuit is too sensitive to be stable, sensitivity can be reduced by lowering the filament and plate potentials of the output tube. (2) The negative bias of the control grid of the input tube, at which the mutual conductance of the unit is a maximum, is directly proportional to the screen grid potential of the input tube. (3) The grid conductance of the input tube is for

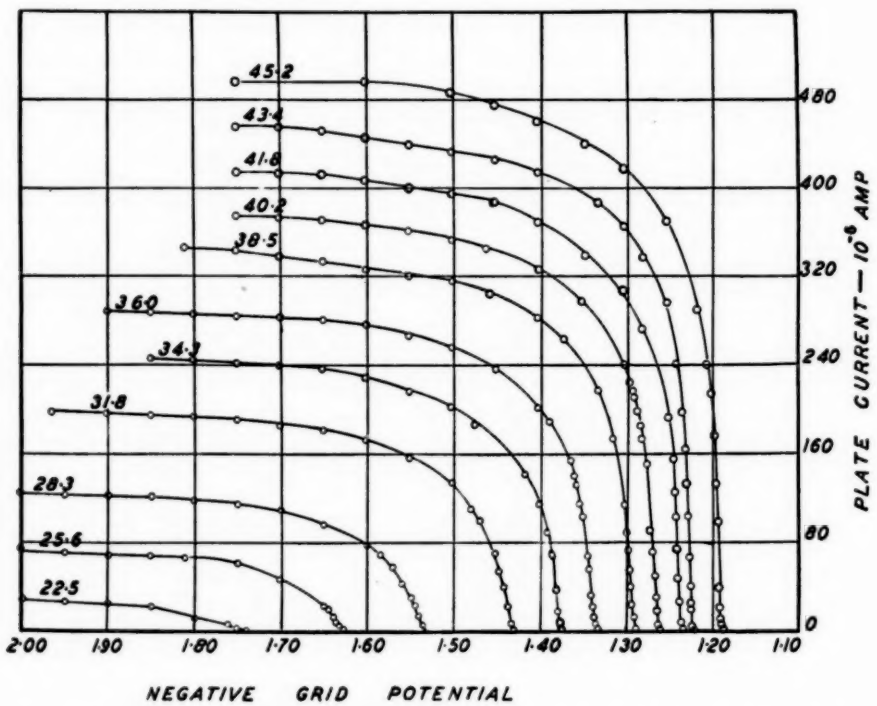

FIG. 4. Showing how the mutual conductance increases with increasing space charge potential of the output tube. The numerical values given are the space charge potentials measured in volts.

practical purposes independent of the screen grid potential. (4) The measured voltage sensitivity of the unit examined was 3×10^{-4} volt/mm, and no appreciable drift was observed. This circuit has since been examined in greater detail and it is the purpose of this communication to show how the voltage sensitivity can be readily controlled and a high input resistance obtained.

Referring to Fig. 1 it will be seen that R_p is the resistance of a grid-filament system and hence under most conditions will be considerably larger than Z_p, a filament-plate system. Thus in order to make the voltage sensitivity as large as possible it is necessary either to decrease R_p or increase Z_p.

Use of a Space Charge Grid to Reduce R_p

An examination of the properties of a UX 222, using the screen grid as a control grid and charging the regular control grid positively to act as a space charge grid, showed that the positive ion grid current increases with increasing space charge potential. The results are shown in Fig. 2 and indicate that the use of a space charge in the output tube should be a satisfactory method of reducing the value of R_p.

In Fig. 3 is shown a circuit which employs this property of the space charge grid to enhance the sensitivity of the amplifier. Fig. 4 shows a family of grid potential *vs.* plate current characteristics of this unit, obtained with different potentials on the space charge. The maximum slope of each of these curves was measured and is plotted in Fig. 2 (circles) where the space charge potentials are used as abscissae. The close relation between the two sets of data plotted in this figure, considered in relation to Eq. (1), indicates that with large space charge potentials $|R_p|\rightarrow|Z_p|$, and shows that the space charge grid offers an effective method of sensitivity control.

Use of Additional Plate Resistance to Gain High Sensitivity

If R_p be compounded of a positive and negative resistance in series their algebraic sum may be adjusted to any desired value.

Hence if the circuit of Fig. 1 be opened between P and G_2 and a resistor of suitable value inserted, the value of R_p may be kept negative and made to approach arithmetic equality with Z_p, with a resulting increase in the voltage sensitivity of the circuit.

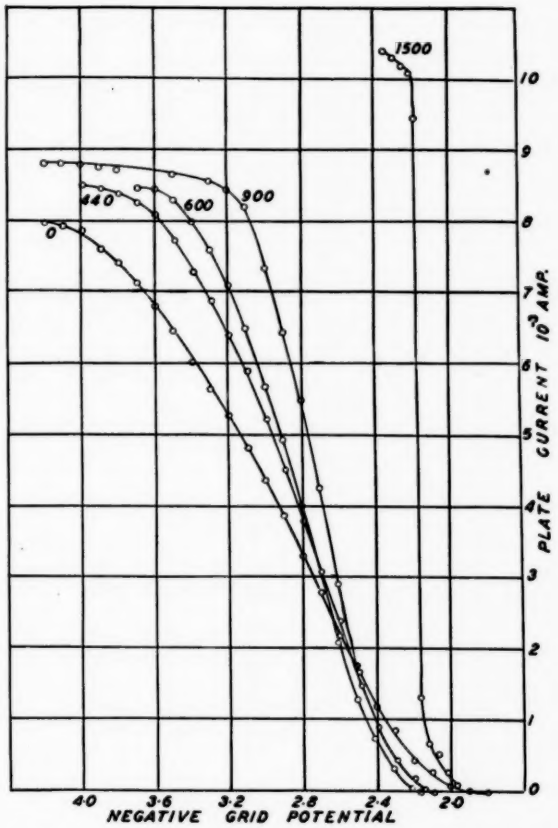

Fig. 5. Showing the effect on the mutual conductance of adding resistance between the plate of the input tube and control grid of the output. The numerical values given are in megohms.

In Fig. 5 is reproduced a family of grid potential *vs.* plate current curves obtained with different resistors in the plate circuit. The data in this case were obtained by using a UX 222 as a triode for the input tube and a 112 A for the output. The plate potential of the input tube, in future to be referred to as the E potential was 12 volts, that of the output tube being 90, with a filament potential of 3.5 volts. This method of sensitivity adjustment is direct and simple.

High Input Resistors

The conditions for maintaining a high input resistance in a UX 222 have been discussed by Macdonald and Tweed.[2] The results of their

[2] Macdonald and Tweed, Physics **4**, 178 (1933).

examination show that with a filament potential of 1.25 volts, a screen grid potential of approximately 10 volts and a plate potential less than that of the screen, the resistance between the filament and grid is in the neighborhood of 5×10^{13} ohms and lies in the positive ion region.

From what has been said of the circuit discussed in this paper it will be apparent that the above conditions may be readily imposed on the input tube and hence the data obtained by Macdonald and Tweed are applicable to this circuit.

In conclusion it may be stated that while the material here presented shows the mechanism of adjustment of the voltage sensitivity to any desired value, one may obtain characteristics suitable for many purposes by the careful choice of tube combinations. A UX 232 used as a triode in the input stage and a 230 in the plate circuit using 22.5 volts on the plate and an E potential of 10 volts behave in a very satisfactory manner.

This work has been carried out in conjunction with the Radium Laboratory of the Manitoba Cancer Relief and Research Institute, established in the Department of Physics, University of Manitoba, and the authors would like to express their thanks to these Institutions for the courtesies which they have extended.

Effect of Circuit Parameters on the Constancy of the Frequency of a Pliodynatron

WILLIAM C. SEARS, *Mendenhall Laboratory of Physics*

(Received March 30, 1933)

A study is made to determine the way in which the frequency of the pliodynatron oscillator depends upon the plate and control-grid voltages. The optimum operating voltages for greatest constancy of frequency are discussed. A new theoretical expression for the frequency of this oscillator is derived. The theoretical frequency variation with plate voltage is shown to be closely in agreement with the experimental variation.

INTRODUCTION

IN 1918 A. W. Hull[1] discussed the method of oscillation of a three electrode tube over its negative resistance characteristic and called the oscillator a "dynatron." Later, in collaboration with E. F. Hennelly and F. R. Elder,[2] he applied the dynatron principle of the four electrode tube and discussed a number of its ingenious applications to radio circuits. He called the four electrode tube oscillator a "pliodynatron."

Moreover, it has been noted that the frequency of the pliodynatron oscillator is inherently quite stable. Since fluctuating voltages may vary the generated frequency of an oscillator, which is not crystal-controlled, it has been the purpose of this paper to make a systematic study of the dependence of the frequency of the pliodynatron oscillator upon the plate and control-grid voltages.

METHOD OF FREQUENCY MEASUREMENT

Fig. 1 shows the arrangement for varying the tube voltages. E is the alternating plate potential and V is the battery potential applied to the plate. In the tuned circuit, C is a fixed capacitance having a leakage resistance S and L is a fixed inductance of resistance R.

Frequency measurements were made by comparison of the test oscillator with a variable standard oscillator of the tuned grid type, with optimum conditions[3] of operating voltages for frequency stability. The variable standard oscillator was calibrated by using the nominal frequency of 1000 cycles per second, given by a microphone hummer as the reference frequency. A small variable air condenser was used as part of the total capacitance, such that its variation from maximum to minimum capacity gave a range of frequency within which the variation of the pliodynatron oscillator under all conditions was known to lie. A small variable inductance in the tuned circuit of the standard oscillator was then adjusted until the middle of the desired range corresponded with the middle of the vernier condenser scale.

In each oscillator circuit there was a loud speaker which made the frequency of the circuit audible. The number of beat notes per second between the two loud speakers was equal to the difference in frequency in the circuits. Slightly

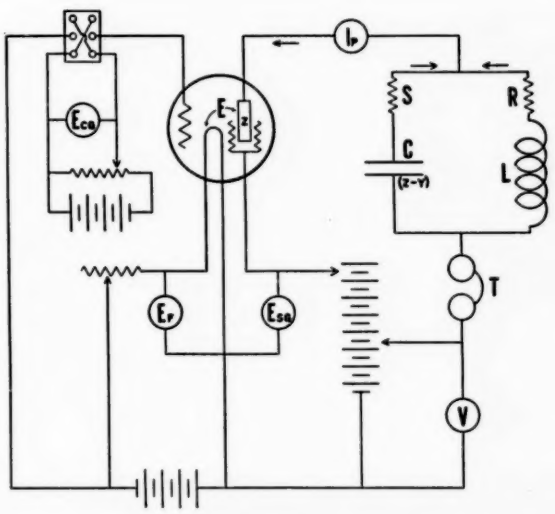

FIG. 1. The pliodynatron oscillator.

[1] A. W. Hull, Proc. I. R. E. **6**, 5–35 (1918).
[2] A. W. Hull, E. F. Hennelly and F. R. Elder, Proc. I. R. E. **10**, 320 (1922).
[3] K. B. Eller, Proc. I. R. E. **16**, 1706 (1928).

increasing the frequency of the standard circuit decreased the number of beats if the test oscillator circuit was at the higher frequency and *vice versa* if it was at the lower frequency. Thus, the measured frequency was the frequency of the standard oscillator plus or minus the number of observed beats per second. The measurements were made in the region of 1000 cycles per second.

The inductance and capacity being held constant, screen-grid, control-grid and plate voltages of the pliodynatron were varied separately and the corresponding frequency change measured by the audible beat method as described above. Applied voltages were then plotted against the corresponding frequencies for all possible combinations of tube voltages. The curves thus obtained showed the voltages for which the fluctuations in these voltages would produce the least variation in frequency. They also indicated what variations in frequency occur under operating conditions other than the optimum.

Experimental Results

Fig. 2 shows the variation of plate current with plate voltage for various control-grid voltages. The full curves represent the oscillatory characteristics and the broken curves the static characteristics, i.e., with the tuned circuit shorted out. The symmetry of these curves is to be noted and also the fact that the positive slope of the oscillatory characteristic disappears with decreasing control-grid voltage.

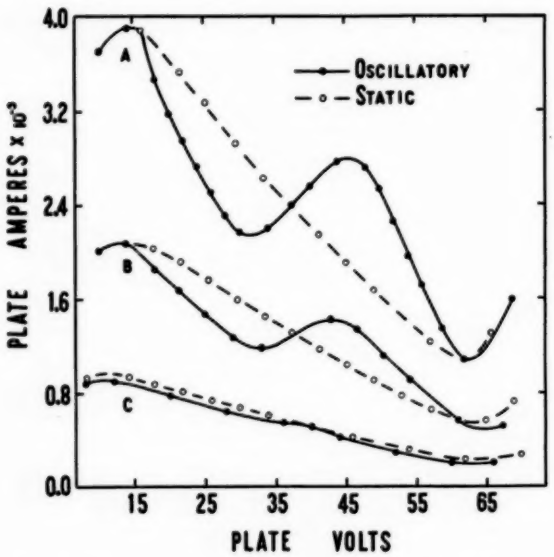

Fig. 2. Plate current as a decreasing function of the plate voltage for the following control-grid voltages: *A*, 9 volts; *B*, 0 volts; *C*, −6 volts. Screen-grid potential = 76 volts. Filament potential = 3.3 volts.

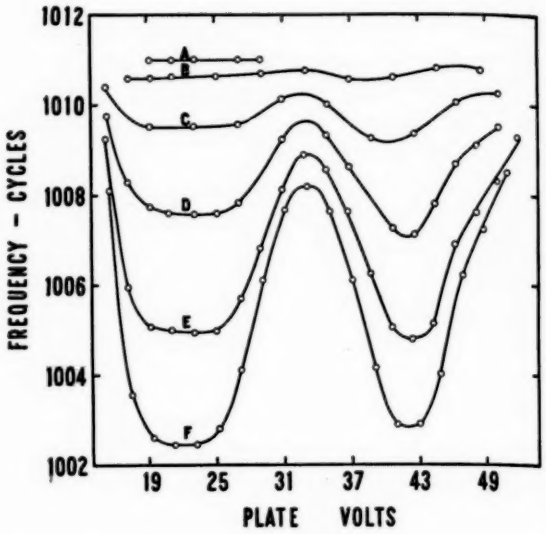

Fig. 3. Variation of frequency with plate voltage for the following control-grid voltages: *A*, −5 volts; *B*, −2.5 volts; *C*, 0 volts; *D*, 3 volts; *E*, 6 volts; *F*, 9 volts. Screen-grid potential = 66.2 volts. Filament potential = 3.3 volts.

In Fig. 3 the frequency is shown as a function of the plate voltage for different control-grid voltages. The curves are of the fourth degree type, but it was found that the symmetry is lost if the screen-grid voltage is less than 45 volts. As the grid voltage is increased negatively to the voltage where oscillations cease, the slope of the corresponding frequency curve approaches zero. Thus, for a high negative control-grid voltage the plate voltage variation of frequency becomes practically zero.

The variation of frequency with plate voltage for various screen-grid and filament voltages is quite similar to that for various control-grid voltages.

Also it was found that the oscillatory and static characteristics became nearly the same for conditions of greatest frequency stability. The plate voltage at which the two characteristics cross corresponds exactly with the voltage for which the central maximum in the frequency occurs.

Theoretical Frequency of the Pliodynatron Oscillator

A theoretical expression for the frequency of the pliodynatron oscillator may now be derived. Since the circuit incorporates no feedback from plate to grid for sustaining oscillations, the filament, control-grid and screen-grid voltages may be considered as constants and the analysis may be confined to the plate circuit. The instantaneous values of the charge on the plate and condenser are z and $(z-y)$, respectively, as shown in Fig. 1. By Kirchhoff's laws,

$$L\ddot{y}+R\dot{y}=V-E, \tag{1}$$

$$(1/C)(z-y)+S(\dot{z}-\dot{y})=V-E, \tag{2}$$

where the differentiation is taken with respect to time. Neglecting transients and choosing the time zero so that the phase of the fundamental in E is $\pi/2$, we may assume the alternating plate potential to be of the form,

$$E=A_0+A_1\cos\omega t+A_2\cos 2\omega t\cdot+\cdots +B_2\sin 2\omega t\cdot+\cdots \tag{3}$$

The fundamental frequency, f, is $\omega/2\pi$.

Let the current through the tube be some function of the plate voltage,

$$\dot{z}=\varphi(E). \tag{4}$$

The differential Eqs. (1) and (2) may be solved for y and $(z-y)$, respectively, obtaining a complex Fourier series for each. The sum of these two series is the value of z, which, on being differentiated, is equal to $\varphi(E)$. Thus,

$$\left.\begin{aligned}\dot{z}=\frac{V-A_0}{R}-\left[\frac{RA_1}{L^2\omega^2+R^2}+\frac{C^2SA_1\omega^2}{1+C^2S^2\omega^2}\right]\cos\omega t-\left[\frac{4C^2SA_2\omega^2+2CB_2\omega}{1+4C^2S^2\omega^2}+\frac{RA_2-2LB_2\omega}{4L^2\omega^2+R^2}\right]\cos 2\omega t+\cdots\\ +\left[\frac{CA_1\omega}{1+C^2S^2\omega^2}-\frac{LA_1\omega}{L^2\omega^2+R^2}\right]\sin\omega t+\left[\frac{2CA_2\omega-4C^2SB_2\omega^2}{1+4C^2S^2\omega^2}-\frac{2LA_2\omega+RB_2}{4L^2\omega^2+R^2}\right]\sin 2\omega t+\cdots\\ \equiv\varphi\left[A_0+A_1\cos\omega t+A_2\cos 2\omega t+\cdots +B_2\sin 2\omega t+\cdots\right].\end{aligned}\right\} \tag{5}$$

By the conventional method for determining the coefficients in a Fourier series, Eq. (5) may be divided into a number of simpler component equations. Since R and S are comparatively small, these equations may be further simplified[4] to become,

$$\left.\begin{aligned}&\frac{1}{2\pi}\int_0^{2\pi}\varphi[A_0+A_1\cos\theta]d\theta=(V-A_0)/R && \text{a}\\ &\frac{1}{\pi}\int_0^{2\pi}\cos\theta\,\varphi[A_0+A_1\cos\theta]d\theta=-[R/L^2\omega^2+C^2S\omega^2]A_1 && \text{b}\\ &\frac{1}{\pi}\int_0^{2\pi}\sin\theta\,\varphi[A_0+A_1\cos\theta]d\theta=[C\omega-1/L\omega]A_1 && \text{c}\\ &\frac{1}{\pi}\int_0^{2\pi}\cos 2\theta\,\varphi[A_0+A_1\cos\theta]d\theta=-[2C\omega-1/2L\omega]B_2 && \text{d}\\ &\frac{1}{\pi}\int_0^{2\pi}\sin 2\theta\,\varphi[A_0+A_1\cos\theta]d\theta=[2C\omega-1/2L\omega]A_2. && \text{e}\end{aligned}\right\} \tag{6}$$

Therefore, as first approximations, $A_2=0$, $\omega=1/(LC)^{\frac{1}{2}}$,

[4] Higher harmonics are being neglected as a first approximation.

$$\frac{1}{A_1\pi}\int_0^{2\pi}\cos\theta\,\varphi[A_0+A_1\cos\theta]d\theta=-(C/L)(R+S) \tag{7}$$

and

$$B_2=-\tfrac{2}{3}(L/C)^{\frac{1}{2}}(1/\pi)\int_0^{2\pi}\cos 2\theta\,\varphi[A_0+A_1\cos\theta]d\theta. \tag{8}$$

For a given plate voltage,

$$V=A_0+RI_0, \tag{9}$$

where I_0 is the mean value of the current from the oscillatory characteristic at the voltage, V, and A_0 is the static plate voltage. The function, $\varphi[A_0+A_1\cos\theta]$, as defined by (4) is the value of the current from the static characteristic at the voltage, $[A_0+A_1\cos\theta]$. By approximate integration of (7), a value of A_1 must be found for a particular plate voltage, V, such that the equation is satisfied. Then B_2 may be computed from (8).

The equation giving the second approximation for the frequency is

$$\frac{1}{\pi}\int_0^{2\pi}\sin\theta\varphi[A_0+A_1\cos\theta+B_2\sin 2\theta]d\theta$$

$$=[C\omega-1/L\omega]A_1. \tag{10}$$

If B_2 is small compared with A_1, (10) may be written

$$\frac{B_2}{\pi}\int_0^{2\pi}\sin 2\theta\sin\theta\varphi'[A_0+A_1\cos\theta]d\theta$$

$$\approx[C\omega-1/L\omega]A_1, \tag{11}$$

where the prime denotes the derivative of the function with respect to its argument. Integrating (11) by parts and using (6c), the expression for the frequency finally becomes,

$$f=1/2\pi(LC)^{\frac{1}{2}}[(A_1^2+B_2^2)/(A_1^2+4B_2^2)]^{\frac{1}{2}}. \tag{12}$$

By determining the values of the amplitudes of oscillation, A_1 and B_2, for a particular V, as described above, the frequency corresponding to this particular plate voltage may be calculated by use of Eq. (12). Thus, by computing frequencies for different plate voltages, it is possible to plot the theoretical frequency as a function of the plate voltage.

Comparison of Theory and Experiment

Inspection of the theoretical and experimental frequency—plate voltage curves of Fig. 4 shows that they are of the same general shape. The plate voltages at which the maximum and the minimum occur are exactly coincident for both curves. The total variation of frequency from the maximum to the minimum is found to be greater experimentally than theoretically. This is probably due to the fact that the frequencies calculated are only correct to second approximations. Thus, the theory suggests the presence of high harmonics in the pliodynatron oscillator, such as to be in agreement with that which F. B. Llewellyn[5] found experimentally.

The theoretical frequencies are approximately 1.6 percent less than the experimental frequencies, which is probably within the limit of experimental error, inasmuch as the accuracy of the reference frequency was not known. The maximum and the minimum plate voltages for which oscillations are sustained are very nearly the same in both cases.

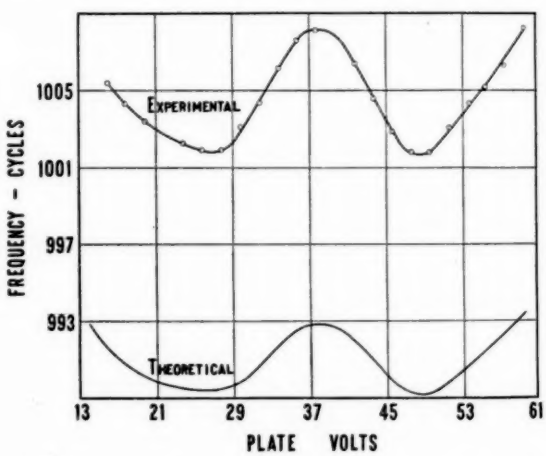

FIG. 4. Comparison of the experimental with the theoretical frequency variation with plate voltage. Screen-grid potential = 75.9 volts. Filament potential = 3.3 volts. Control-grid potential = 6 volts.

[5] F. B. Llewellyn, Bell Sys. Tech. J. **11**, 67–100 (1932).

Conclusions

The general agreement between the theoretical and experimental frequency variation with plate voltage, which is indicated in Fig. 4, serves to verify the theoretical equation for the frequency of the pliodynatron as previously developed.

The frequency of this oscillator is very nearly independent of fluctuations in the operating voltages for the U.X.-322 tube, if the screen-grid is maintained at a potential of approximately 60 volts, the filament at its rated voltage, and the control-grid as highly negative as will sustain oscillations. Under these conditions the plate voltage variation of frequency becomes practically zero. Positively increasing the control-grid potential greatly increases the total variation in frequency from the maximum to the minimum.

The author wishes to express his sincere appreciation to Professors Alva W. Smith and L. H. Thomas, under whose direction this work was completed.

A Photoelectric Valve

JAKOB KUNZ AND J. T. TYKOCINER, *University of Illinois*
(Received March 13, 1933)

The object of this experimental investigation was to determine the nature of the valve effect. After the description of the valve some characteristic and photometric curves are given. Sensitivity curves are then described which show the relation between the wave-length and the photoelectric current per unit of light energy. These curves show distinct maxima, like ordinary photoelectric cells; this character of the sensitivity curves support the theory that the effect is primarily a photoelectric phenomenon connected with space charges. Other assumptions are shown to be untenable. Some additional phenomena, expecially of the dark current, and experiments with various modifications of the valve are reported.

THE photoelectric device discovered almost simultaneously by ourselves[1] and by Hyatt,[2] has been further studied by V. M. Albers.[3] Since 1925 we have made further measurements with the same apparatus, which we called a photoelectric valve and we propose to describe the results of these measurements. The object of this research was in the first place to find an explanation of the phenomenon, to increase if possible, the action of the cell, to determine whether under certain conditions there may exist besides the photoelectric effect other phenomena, such as conduction, re-emission of electrons, or ionization, and to study some variations in the construction of the cell, such as the dimensions of the cell, the effect of different glasses and different alkali metals.

CONSTRUCTION OF CELLS AND EXPERIMENTAL ARRANGEMENT

The cells used were of the same type as those described by Albers. The tube with the electric connections is shown in Fig. 1. It is provided with an oxide-coated filament. It has to be carefully cleansed with solutions of potassium-bichromate, nitric acid and sodium hydroxide. The alkali metal which is repeatedly distilled in a high vacuum is finally poured into the evacuated valve, which is then heated in a furnace 3 hours at 300 or 450°C according to the glass used. Meanwhile the filament is heated and the highest vacuum obtainable is maintained during this process. After about 3 hours the cell is sealed off. After cooling, the alkali metal remaining in a small bulb outside the valve is distilled or poured into the anode bulb, from there it is distilled onto the walls of the connecting tube, and then driven back into the anode bulb by means of Bunsen flames or the electric furnace. The valve is then placed in a light-tight box, having several slits for the illumination of various parts of the valve. The source of light was a 400 watt stereopticon lamp, in a lamp house, which was cooled with a blast of air. The light from the lamp was focussed onto a diaphragm and from there made parallel so as just to cover the connecting tube of the cell. The intensity of the light was varied by means of a

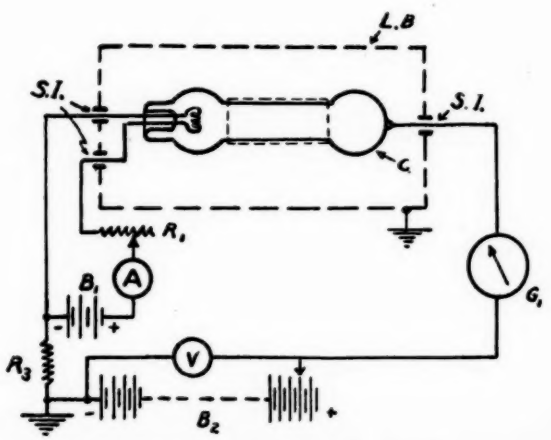

FIG. 1. Tube and electrical circuits

[1] Tykociner and Kunz, Science **59**, 320 (1924).
[2] Hyatt, Phys. Rev. **23**, 501 (1924).
[3] Albers, Phys. Rev. **26**, 671 (1925).

rotating sector disk placed near the diaphragm. The intensity of the light was measured by a Weston illuminometer. The cell was in a simple electric circuit containing a battery of 430 volts, a galvanometer, and a safety resistance, all in series. In order to reduce losses in the circuit as much as possible, all insulation between the cell and the measuring instrument was of sulphur or paraffin. All wires were carefully shielded to reduce the effect of stray electrostatic fields. Monochromatic light was obtained by means of a Kipp and Zonen double monochromator which was adjusted so as to give maximum output consistent with purity of color. The energy of the monochromatic beam was determined by a Coblentz thermocouple of 12 ohms resistance and a corresponding high sensitivity galvanometer. The monochromator was calibrated by means of a constant deviation spectroscope whose wavelength scale was checked against the lines in a helium glow discharge. The currents of the cell, when illuminated by monochromatic light, were of course smaller than those obtained by white light and had to be measured by means of an electrometer. The cell or valve was in series with a battery and a resistance made of a graphite pencil mark on a piece of Bakelite. The ends of this resistance were connected with the quadrants of the electrometer. In order to obtain a large effect, the filament was wound into a large coil, and the valve was made somewhat shorter and wider than before, the tube connecting the bulbs at the end was about 10 cm long and 2 or 2.5 cm wide. The temperature of the filament was kept so low that its light had no photoelectric effect on the tube. The film of the alkali metal on the walls of the tube was of different thickness in different experiments; sometimes it was visible and at other times invisible.

Characteristics of the Cell

With the filament current kept constant at 0.90 amp., and a film of potassium which was just visible in strong light, the potential (anode potential) between anode and cathode was varied between 0 and 270 volts and the curves of

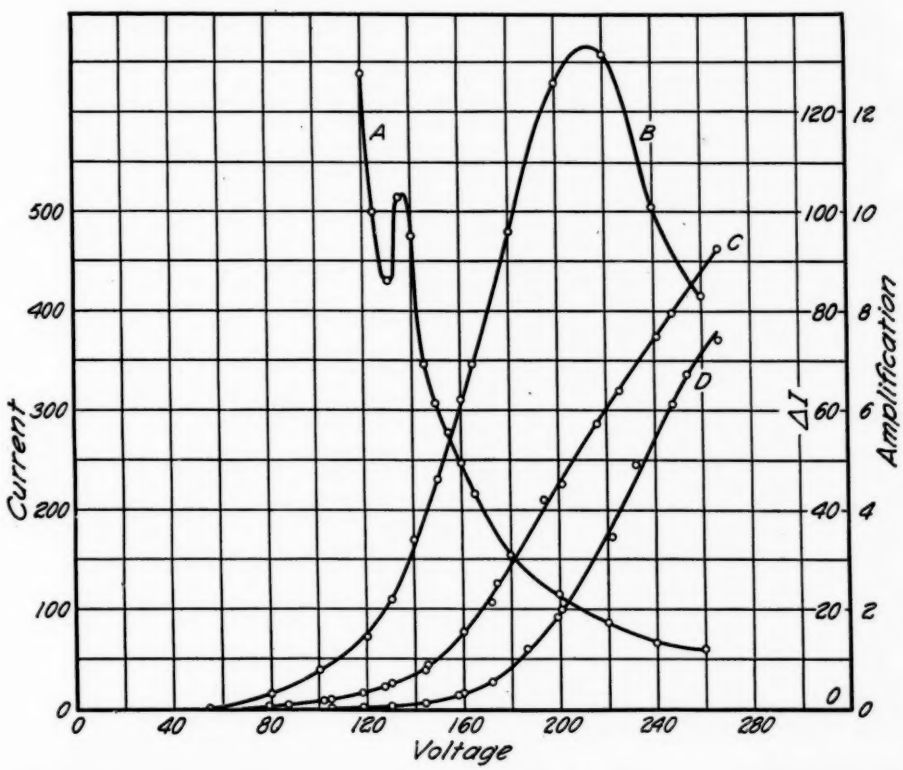

FIG. 2. Current-voltage characteristics of tube. *A* shows the ratio i_e/i_d, *B* the difference between i_e (curve *C*) and i_d (curve *D*).

Fig. 2 were obtained. Curve D represents the dark current i_d, C the curve obtained with light of about 2 footcandles, i_e, B the curve $i=i_e-i_d$, and A the curve i_e/i_d or the amplification voltage curve. It will be observed that these characteristics are almost identical with those obtained by Albers, including the strange maximum and minimum points on the i_e/i_d curves. Very similar results were obtained for invisible films. The dark currents are here rather large. At 200 volts the dark current was 4.60×10^{-8}, the light current 10.55×10^{-8} amp. But in later experiments with films quite transparent, but of a misty gray appearance the dark current became negligible as compared with the light current.

Current and Illumination

Many experiments were carried out in order to find the relation between light intensity and photoelectric current. The film of potassium metal though quite translucent, showed the characteristic colors of interference. The maximum light intensity was 2 footcandles; the filament current was 1.1 amp. Fig. 3 gives the results of one series. Curve C shows the dark characteristic of the cell, B the current voltage relation under the action of light, and A represents the relation between illumination (2 footcandles = 100 percent) and current. It is evident that the dark current is very small, and that the current is nearly proportional to the light intensity. Thicker films yield still better straight lines and currents are sometimes obtained which are much larger than those from ordinary photoelectric cells. As a rule the same curve was obtained when the illumination increased and when it decreased. But occasionally after illumination there remained a considerable dark current. In trying to obtain the proper distribution of potassium on the connecting tube, it was noticed that if the filament bulb was illuminated along with the connecting tube, there was a considerable increase in the current through the cell. The cell was placed in a box with two partitions in it. These partitions were so arranged that the filament bulb, the connecting tube and the anode bulb were each in a separate light-proof compartment. Windows over the filament bulb and connecting tube could be opened and closed. In Fig. 4 the window opening to the connecting tube

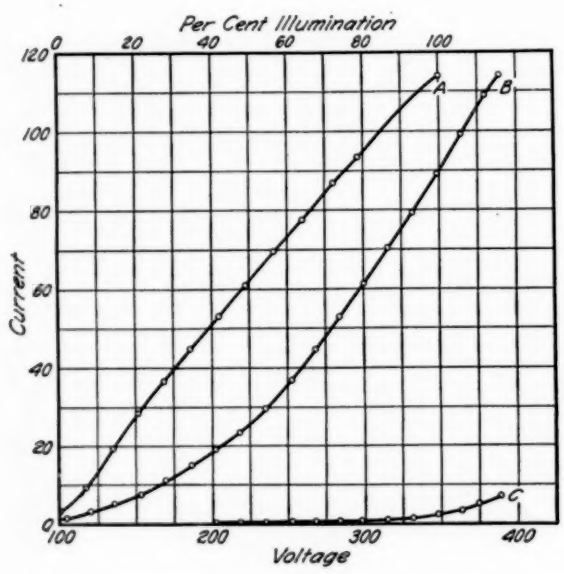

Fig. 3. Current-voltage curves. Curve A current *vs.* illumination, curve B for illuminated cell, curve C gives the current when the cell is dark.

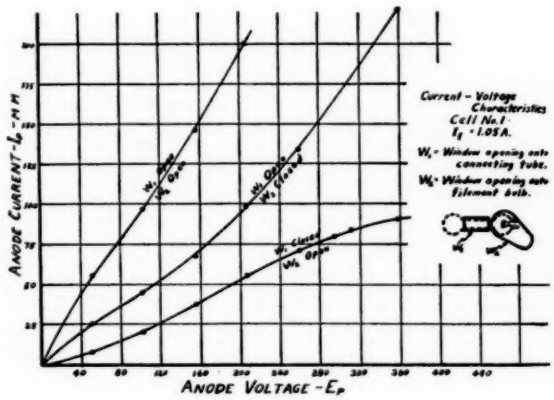
Current - Voltage Characteristics
Cell No. 1
I_f = 1.05 A.
W_1 - Window opening onto connecting Tube.
W_2 - Window opening onto filament bulb.
Anode Current - i_p m m
Anode Voltage - E_p

Fig. 4. Current-voltage curves with cell partially illuminated.

is designated as w_1 and the window opening to the filament bulb was w_2. The largest current is obtained when both windows are opened, the smallest current when w_1 is closed and w_2 open. It is seen that the opening of the window over the filament bulb increases the current to a marked degree. For a given voltage between cathode and anode, the anode current increases with increasing filament current within a certain range (see Fig. 5). Light falling on the filament increases the emission of electrons which may

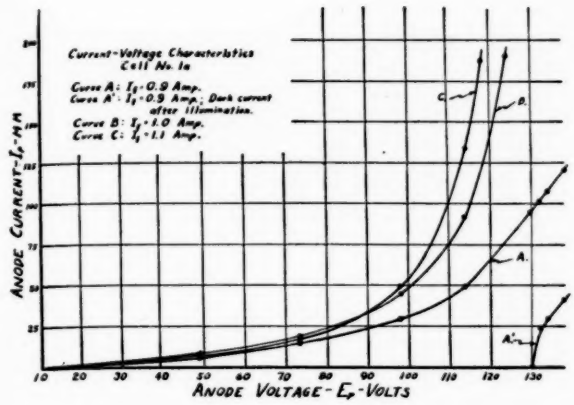
Current-Voltage Characteristics
Cell No. 1a
Curve A: I_f = 0.9 Amp.
Curve A': I_f = 0.9 Amp.; Dark current after illumination.
Curve B: I_f = 1.0 Amp.
Curve C: I_f = 1.1 Amp.
ANODE CURRENT - I_p - MM
ANODE VOLTAGE - E_p - VOLTS

FIG. 5. Current-voltage curves with various filament currents.

account for a part of the increase of the anode current, when w_2 is opened. This however does not explain the whole effect, because it does not explain the reason for the current when w_1 and w_2 are both open, being considerably larger than the sum of the currents when w_1 and w_2 are opened separately. We shall find the effect is partly due to the decreasing of the space charge in the bulb and around the opening into the connecting tube.

COLOR SENSITIVENESS

The first explanation of the action of the photoelectric valve consisted in the assumption that it was a photoelectric and space charge effect. But the measurements of V. M. Albers seem to contradict this assumption since in the wave-length, specific deflection curve,—he found no maximum at 4400A where the ordinary potassium cell shows a maximum. It became therefore necessary to repeat these experiments and to measure the energy of the light source in the region between 4100A and 5000A very accurately. The energy in this region was so small, however, that the direct method of measurement with a thermopile was inaccurate. To overcome this it was decided to determine as accurately as possible the distribution of energy, experimentally in the region between 5000A and 7000A. These data were used to draw an empirical curve for which a mathematical expression was found, this expression was then used to determine the energy of the region between 4100A and 5000A. For 3 values of the lamp current, the energy E in the spectrum was found to correspond accurately to the formula: $E = A\nu^6 e^{-b\nu}$ where A and b are constants, and ν the frequency. The results are plotted in the curves B and C of Fig. 6. The points shown are

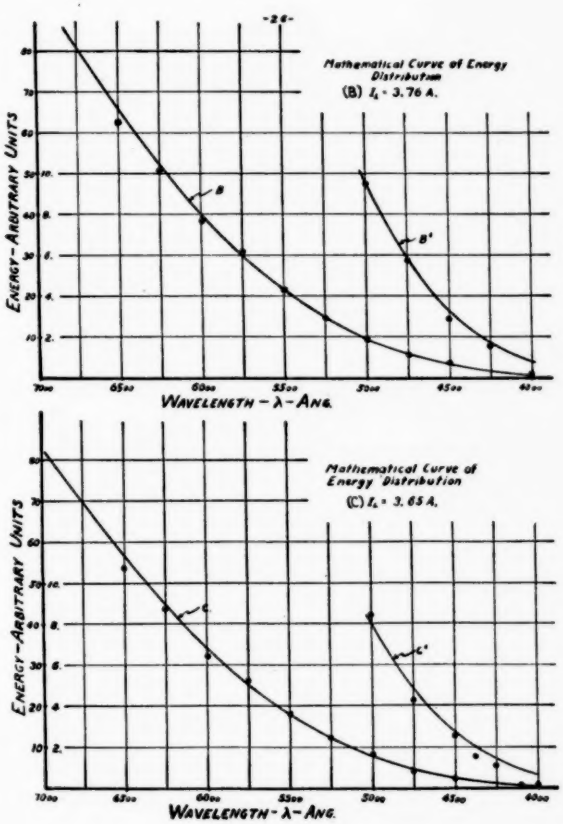
Mathematical Curve of Energy Distribution
(B) I_f = 3.76 A.
ENERGY - ARBITRARY UNITS
WAVELENGTH - λ - ANG.
Mathematical Curve of Energy Distribution
(C) I_f = 3.65 A.
ENERGY - ARBITRARY UNITS
WAVELENGTH - λ - ANG.

FIG. 6. Energy distribution in light from lamp.

the points obtained experimentally; those used to draw the curves, not being shown. B' and C' are portions of the same curves with their ordinates drawn on an enlarged scale. The color sensitivity was determined for several cells, whose films, had a grayish color, and whose dark current was small, and sensitivity for wall light intensities large. Fig. 7 contains the galvanometer deflections of the current as function of the wave-length. The lower curve which is practically parallel to the wave-length axis, represents the dark current. In order to find the relative sensitivity of the cell it was only necessary to divide the magnitude of the current at a certain wave-length by the energy in the beam at that

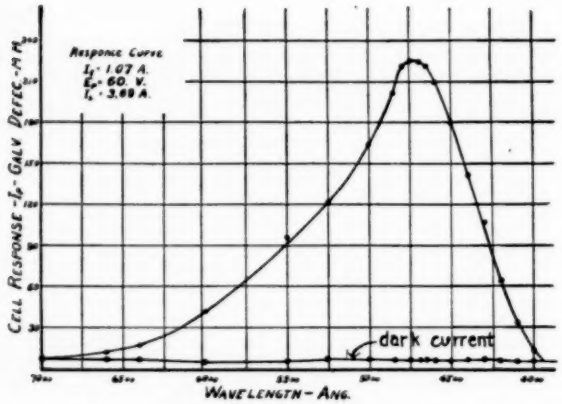

FIG. 7. Color sensitivity (uncorrected) potassium cell.

wave-length. Anode potentials between 50 and 60 volts were used. The results are plotted in the curves *A*, *B* and *C* of Fig. 8 corresponding to 3 different lamp currents, (I_L) while for comparison curve *D* shows the relative sensitivity of potassium in an ordinary soft glass photoelectric cell as determined by Miss Seiler.[4] There are

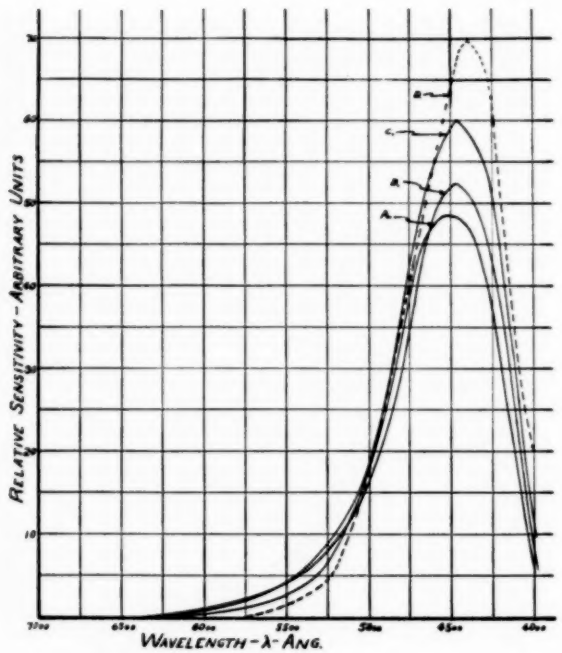

FIG. 8. Color sensitivity (corrected) potassium cell. Relative sensitivity current. Photoelectric valve.

	Anode potential	Lamp current
Curve *A*	52 v	3.81A
Curve *B*	52 v	3.69A
Curve *C*	60 v	3.69A

Curve *D*—For ordinary potassium cell (by Miss Seiler).

[4] Seiler, Astrophys. J. **52**, 129 (1920).

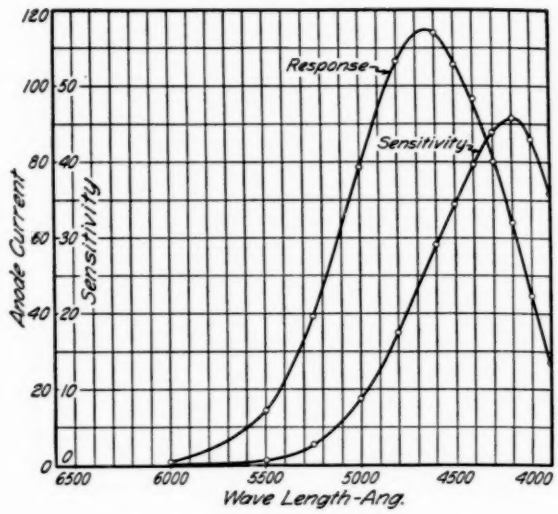

FIG. 9. Color sensitivity; sodium cell.

small differences between these curves. The sensitivity of the ordinary photoelectric cell has a sharper maximum at 4400A than the present valve whose maximum lies at 4450 or even at 4470A. This difference may partly be due to inaccuracy, partly due to the fact that the maximum even for ordinary photoelectric cells varies within a small interval, depending for instance on the inert gas in the cell. Moreover for thin films of alkali metals deposited on metal surfaces in a high vacuum, Ives[5] found that the selective effect only occurs for certain thicknesses of film; the effect is absent for very thin films and for thick films of the pure metal. This may explain the fact that Albers did not find any indication of a maximum in his sensitivity curves. The maximum in the sensitivity curve of the potassium film is evidence in favor of the assumption that the valve effect is a photoelectric effect.

This idea was to be tested by means of sodium films. Cells were therefore prepared containing sodium. In order to get rid of all occluded gases the first cell was heated to about 400°C, a temperature at which the glass was slightly attacked by the sodium vapor and showed a beautifully golden color after heating. The characteristic curves and the photometric curve, illumination against anode current, are quite analogous to the corresponding potassium curves. The maximum

[5] Ives, Astrophys. J. **60**, 209 (1924).

appeared in this cell at 4500A while the maximum of an ordinary sodium cell occurs at 4200A. This is at least partly due to the absorption of light by the colored glass. Other cells were prepared at a lower temperature without the glass being colored and the maximum shifted indeed toward the violet end of the spectrum, occurring at 4200A as shown in Fig. 9, a point which exactly coincides with the maximum sensitivity of ordinary sodium photo-cells.

Theory of the Photoelectric Valve

Three possibilities present themselves if we attempt an explanation of the present phenomenon.

(1) The increased current due to illumination may be due to an increase in the reflecting power of the alkali film surface for electrons.

(2) Leakage currents may exist due to the finite resistance of the film and the increase in current may be caused by a decrease in the ohmic resistance due to illumination.

(3) The effect might be due entirely to the accumulation of a negative charge on the alkali film and its discharge when illuminated. In other words, the observed effect may be due to space charge and photoelectric action.

Against the first possibility speaks an investigation by Millikan and Barber,[6] who showed that no direct reflection of electrons occurs for voltages lower than the ionizing potential for the surface. For voltages greater than this value it would be difficult to differentiate experimentally between electrons which are directly reflected and secondary electrons due to impact of primary electrons. The alkali film is always negatively charged so that electrons strike it with relatively low velocities probably too small to cause ionization.

In order to test the second assumption a tube of the form shown in Fig. 10 was constructed. Two platinum wires were sealed into the tube at C and D and heavy deposits of silver S and S' were formed on the sides of the tube to connect with the platinum electrodes. A silver wire was sealed to platinum wires A and B through the center of the tube. This wire was kept at a sufficiently high potential with respect to C and D to collect any photoelectrons which might be emitted. Ives and Johnsrud[7] have shown that rubidium films, although quite invisible, are conducting and that the ohmic resistance of such films apparently decreases when illuminated. The experimental tube used by Ives and Johnsrud did not permit of differentiation between currents due to photo-emission and currents due to ohmic resistance while the tube used in this investigation permitted of such a differentiation. Potassium was distilled into the tube by the usual method, and the portion of the tube between C and D was put in series with an electrometer of sensitivity of about 10^{-11} amp. per mm. The current remained too small to be measured, even when the tube was strongly illuminated. The procedure was repeated for thicker films until finally quite thick deposits of grayish appearance were tried. In no case could a current be detected with the electrometer for 400 volts potential difference. Upon close examination it was found that these visible films consisted of small globules insulated from one another. It is not improbable then that the invisible films also, due to surface tension, consist of tiny globules separated by regions in which no deposit occurs. This failure of thin potassium films to conduct, either when dark or illuminated, ruled out the second possibility.

The mechanism of the valve effect was further investigated with a special tube shown in Fig. 11. The usual form of tube was used except that a platinum electrode was sealed into the connecting tube and one-half of the inner surface was silvered in the usual way. The potential difference

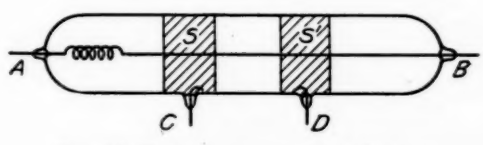

Fig. 10. Tube to test ohmic resistance.

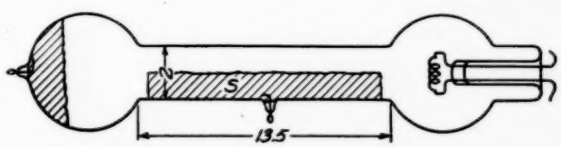

Fig. 11. Modified tube. S is silvered surface.

[6] Millikan and Barber, Proc. Nat. Acad. Sci. **7** (1921).

[7] Ives and Johnsrud, Astrophys. J. **62**, 309 (1926).

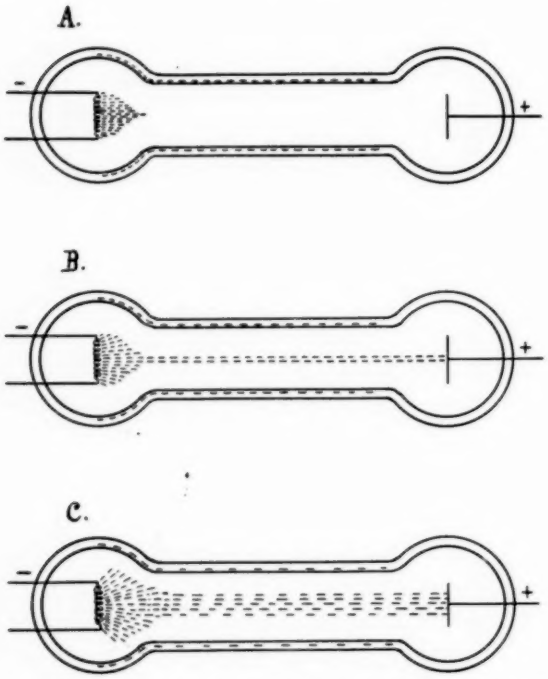

FIG. 12. Influence of illumination on space charge and anode current.

between the silvered surface and the filament was measured by an electrometer, the silvered surface being connected to the needle, while a fixed small potential was maintained between the quadrants. With a potential across the tube, but with no filament current, the electrometer showed no difference of potential. As soon as the filament current was turned on, the surface S became negatively charged with respect to the filament. If now the surface S with a thin potassium film was illuminated, the negative charge decreased and the decrease became greater as the intensity of the incident light became greater. It was impossible to reduce the negative charge to zero even with quite intense illumination.

The space charge and the photoelectric effect seem to interact in the following way: Suppose the tube to be initially dark and the filament giving off electrons. If a voltage be applied across the tube, these electrons begin to move toward the anode. The electron stream broadens out and fills the entire tube. Some of the electrons strike the walls of the tube and remain there charging the film negatively.

The surface charge thus collected on the inner wall may entirely stop the passage of electrons from the cathode to the anode. Instead of flowing in a uniform stream through the tube the electrons form a dense cloud close to the cathode as indicated diagrammatically in Fig. 12A.

If now the film be feebly illuminated, a photoelectric current is set up from the surface which decreases its negative charge and reduces the space charge. This makes it possible for a concentrated beam of electrons to flow along the axis of the tube as illustrated in Fig. 12B. The remaining negative charge on the walls limits the intensity of the anode current. The rate at which electrons strike the film now equals the rate at which they leave under the action of the light, if we assume there is no secondary emission and no direct reflection of electrons. If the intensity of illumination is increased an additional photoelectric current is set up from the surface. This decreases still more its negative charge and causes a new balance to be attained at a lower negative potential. A larger current can now flow through the tube with electrons moving across a larger area of the tube's cross section as indicated in Fig. 12C.

Ives[8] also showed that invisible alkali films were photoactive. Of course if the ordinary valve be illuminated without a filament current, no photocurrent can be detected for any voltage for the potassium film is then well insulated and immediately develops a sufficiently positive potential to prevent the escape of any electrons.

SECONDARY EFFECTS OBSERVED IN THE VALVE

The dark current of most cells was negligible under the action of the voltage across the cell. Illuminating the connecting tube would produce a considerable current. In several cases, especially with Pyrex tubes, the current continued to flow at a reduced magnitude when the light was shut off, but still at a value much larger than the original dark current. This current is shown in curve A' of Fig. 5. If the light was turned on again the current increased to the value which it had before when illuminated. This effect begins at a definite voltage, and increases with increasing potential difference. It was absent in

[8] Ives. Astrophys. J. **60**, 209 (1924).

many tubes and as a rule for higher filament currents.

Another secondary effect is a transient dark current which was also observed only in rare cases. When the voltage E_p between anode and cathode had reached a certain value while the cell was dark, there was at first a small short pulse of current which suddenly stopped. From 10 to 20 seconds after applying E_p a large charge of electricity would pass through the system, indicated by a single violent swing of the galvanometer, which afterwards registered a small steady current. If the connecting tube was illuminated the current would increase considerably, then when the light was shut off, the current would drop to some value a little below that which it had before being illuminated. By interrupting the applied voltage for a moment and then connecting it again, the cycle could be started from the beginning. The action is indicated in Fig. 13. About a minute after the

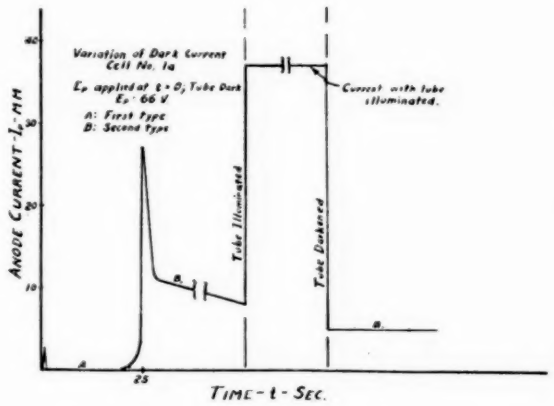
Variation of Dark Current
Cell No. 1a
E_p applied at t = 0; Tube Dark
E_p = 66 V
A: First Type
B: Second Type
Current with tube illuminated.
Tube Illuminated
Tube Darkened
ANODE CURRENT - I_p - MM
TIME - t - SEC.

FIG. 13. Peculiar variations of dark current.

first discharge, it was observed a few times, the current through the cell suddenly rose to a value considerably greater than the first discharge; after the second rise the current decayed slowly. Sometimes however the current would not drop to a constant value, but show a periodic character as indicated by Fig. 14. The period of the galvanometer was longer than the interval between discharges, so that it was impossible to tell whether the current dropped to zero between discharges or whether it had some definite value. The first discharge was usually much stronger

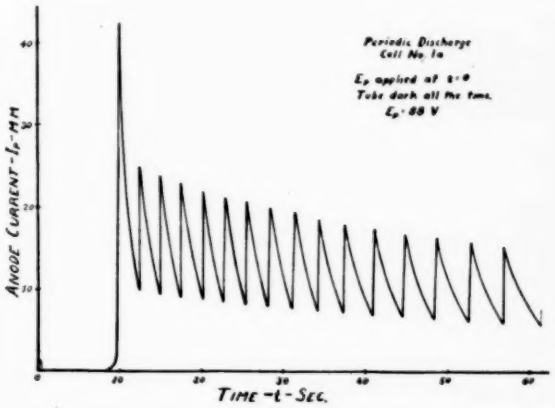

FIG. 14. Periodic dark current.

than the following ones. The magnitude of the discharges gradually decreased and the period increased the longer they were observed on any one test. They usually died out after several minutes, but could be started again by interrupting the voltage for an instant. Sometimes the swing of the galvanometer would be between 53 and 66 millimeters and the frequency would be 36 per minute. When the discharges died out, the galvanometer would indicate a small current of 3 or 4 millimeters. If the connecting tube was illuminated during the oscillation, the current increased to a large value, but when the tube was darkened the oscillations started over again. This phenomenon resembles that of a leaky grid in a three electrode tube. There may be creepage along the surface of the glass or minute discharges may take place between adjacent droplets of potassium in the film of the connecting tube.

EXPERIMENTS WITH DIFFERENT TYPES OF VALVES

The cells so far used were made of Jena glass. Similar cells were constructed of Pyrex glass; they have about the same properties as the previous cells, except that the dark current was zero up to about 125 volts and then increased rather rapidly. The Pyrex photometric curve showed a slight curvature. But other cells gave a straight line over long intervals of intensities except for low intensities; it even happened that no deflection could be obtained for light intensities of less than 8 f.c. Smaller cells have about

the same characteristics as larger cells but they require much higher voltages for the same current. The current for the same voltage and filament current seems to be proportional to the cross-sectional area and inversely proportional to the length of the connecting tube. Several tubes were made with sodium films. The characteristics were similar to those obtained by potassium cells. The color sensitivity of the sodium cells has already been mentioned.

This investigation has been greatly assisted by grants from the National Research Council and the graduate school of the University of Illinois. We wish also to thank Messrs. H. N. Swenson and J. H. Armstrong for valuable assistance in performing the measurements.

The Theory of the Psychrometer. I. The Mechanism of Evaporation

J. HOWARD ARNOLD, *Department of Chemical Engineering, Massachusetts Institute of Technology*

(Received March 8, 1933)

Neither the diffusional theory of Maxwell nor the convectional theory of August is capable of representing adequately the processes of evaporation and heat transfer occurring at the wet bulb. An examination of these processes with the aid of the Reynolds analogy between heat and vapor transfer by convection on one hand, and fluid friction on the other, indicates that the correct theory consists of a combination of the two older theories, in which a mechanism of convection plus conduction is postulated for both heat and vapor transfer. When the thermal diffusivity is equal to the material diffusivity, a special case occurs, for which all three theories give the same result. This condition is approximately satisfied for the case of water evaporating into air; other gases or liquids must therefore be used to discriminate among the various theories. Experiments with water and four organic liquids show that the new theory represents the facts very accurately, and may be made the basis of a sound system for the reduction of psychrometric observations.

HUMIDITY measurements in engineering and meteorological practice are made almost exclusively with the wet-bulb hygrometer, which affords a simple, reliable means for such determinations. Its use dates back to Hutton, about 1792. Although over a hundred papers have dealt with this instrument, no complete, accurate theory has yet been proposed, and present psychrometric practice must be based on semi-empirical tables and equations. It is the purpose of this paper to analyze the processes of heat transfer and evaporation occurring at the wet bulb, and from a consideration of the mechanism of these processes to develop a complete, accurate, physically correct theory.

Two distinct theories of the psychrometer have been proposed: the convection theory, usually associated with the name of August, and the diffusion theory of Maxwell. Both predict the same (correct) *form* of the humidity-temperature relationship; because of their physical incompleteness, neither gives a correct value for the proportionality constant. Empirical correlations of observations by many workers, for the system water-air, have demonstrated the constancy, at a given air velocity, of the ratio

$$\mathbf{A} = (p_w - p_a)/P(t_a - t_w) \qquad (1.01)$$

in agreement with both the convection and the diffusion theory. P is the total pressure, p the partial pressure of vapor, and t the temperature; the subscripts a and w refer to conditions in the air stream and at the wet-bulb surface. The principal concern of psychrometric theory is therefore the prediction of the correct value of the constant **A** under all conditions encountered in practice.

The convection theory was advanced, with but slight variation in form, by Gay-Lussac[1] and Ivory[2] in 1822, by August[3] in 1825, and by Apjohn[4] in 1835. Its basic assumption, as stated by Ivory, is that ". . . all the air that comes in contact with the wet bulb is continually saturated with vapor, and likewise that all the heat necessary for feeding the evaporation is furnished by the same air." Starting from this assumption, a psychrometer equation may be derived easily. The sensible heat lost by a particle of unit mass, on coming in contact with the wet bulb, is $C(t_a - t_w)$. The particle contains $1/M_a$ mols of air, and the mol-fraction of water vapor is increased from p_a/P to p_w/P; the latent heat required for the saturation of the particle with moisture is therefore $M_v\lambda(p_w - p_a)/PM_a$. Equating these heat quantities,

$$\mathbf{A} = (p_w - p_a)/P(t_a - t_w) = M_aC/M_v\lambda. \qquad (1.02)$$

[1] Gay-Lussac, Ann. Chim. Phys. **21**, 82 (1822).
[2] Ivory, Phil. Mag. **60**, 81 (1822).
[3] August, Ann. d. Physik **5**, 65 (1825).
[4] Apjohn, Phil. Mag. **6**, 182; **7**, 266, 470 (1835); **9**, 187 (1836).

M_aC is the molar specific heat of air, $M_v\lambda$ the molar latent heat of the vapor. This is the equation of the convection theory.

Though the proponents of the convection theory apparently were aware of the weakness of its foundations, the objections were overshadowed by the formal correctness of Eq. (1.02), and its consequent agreement with experiment. However, in 1845 Regnault[5] showed that the value of **A** is greatly influenced by the surroundings—an effect due primarily to radiation errors—and recommended that its value be determined empirically, a procedure which has since been followed.

August had assumed the existence of a quiescent film of fully-saturated air around the wet bulb, which interacted with the surrounding partly-saturated air by a process of convection. Directly opposed to the convection theory is the diffusion theory proposed by Maxwell,[6] who postulated that the rates of evaporation and heat transfer were limited by the slowness of diffusion and thermal conduction through the film around the bulb, and neglected the convection processes outside the film. It is now recognized,[7] however, that neither hypothesis is entirely correct; the film is not fully saturated, nor can the effect of convection be neglected. In the theory to be developed below, both convection and conduction (diffusion) will be considered; it is therefore necessary to derive equations for both transfer mechanisms.

Heat Transfer by Convection

Because of the incompleteness of the theory of turbulent fluid motion, it is not possible to formulate directly a theory of convectional heat transfer. However, an analogy between heat transfer and friction (momentum transfer), suggested by Osborne Reynolds,[8] has proved very useful. Consider a particle of unit mass, moving between two points of temperatures t_a, t_b, and mean forward velocities u_a, u_b. The heat transferred amounts to

$$Q = C(t_a - t_b). \tag{1.03}$$

If F is the frictional force per unit area,

$$F = (u_a - u_b)/A\theta \tag{1.04}$$

since the impulse $F\theta$ equals the momentum change; θ is the time during which F is exerted on an area **A** by the particle. From the definition of the thermal conductance in the turbulent region, h_c,

$$(Q/A\theta)/(t_a - t_b) = h_c = FC/(u_a - u_b). \tag{1.05}$$

The shearing force F is transmitted through the film by viscous friction, to which Newton's definition of viscosity applies:

$$F = Z(du/dx) = Z(u_b - u_w)/B = Zu_b/B \tag{1.06}$$

since u_w, the velocity at the wall, is zero. Z is the film viscosity, B the film thickness, and u_b the fluid velocity at the outer boundary of the film. Combining Eqs. (1.05) and (1.06),

$$h_c = CZu_b/B(u_a - u_b) = CZr/B(1 - r), \tag{1.07}$$

in which r is written for the velocity ratio u_b/u_a.

Heat Transfer by Conduction

The rate of heat transfer by conduction is given by Newton's law of cooling: (k = thermal conductivity)

$$Q/A\theta = k(dt/dx) = (k/B)(t_b - t_w) \tag{1.08}$$

dt/dx, the temperature gradient in the film, being replaceable by $\Delta t/B$ when the gradient is constant throughout; t_b is the temperature at the film outer boundary, t_w at the liquid surface. The film conductance, by definition, is

$$h_f = (Q/A\theta)/(t_b - t_w) = k/B. \tag{1.09}$$

Heat Transfer by Convection and Conduction

The thermal conductances are given by Eq. (1.07) for the turbulent zone and Eq. (1.09) for the film. By their combination, an expression may be derived for the rate of heat transfer from the fluid stream to the liquid surface. Adding resistances,

[5] Regnault, Ann. Chim. Phys. **15**, 201 (1845); **37**, 257 (1853).

[6] Maxwell, Article "*Diffusion*," *Encycl. Brittanica* **7**, 218 (1871), Ninth Edition, Edinburgh; *Sci. Papers* **2**, 636 (1890), University Press, Cambridge.

[7] Pannell, Brit. Advisory Comm. Aero., Rep. and Mem. **1**[2], 243 (1916–7).

[8] Reynolds, Phil. Trans. Roy. Soc. **A190**, 67 (1897).

$$1/h_g = 1/h_f + 1/h_c = B/k + B(1-r)/rCZ. \quad (1.10)$$

Solving, the overall conductance is obtained in terms of the film conductance:

$$h_g = (k/B)(CZ/k)/[CZ/k + (1-r)/r]. \quad (1.11)^9$$

Material Transfer by Diffusion

The basic differential equation governing diffusion through films has been derived by Maxwell; its integration was first performed by Stefan[10] and generalized by Chang.[11]

$$-dy_1/dx = (1/D)(y_1 y_2)(u_1 - u_2). \quad (1.12)$$

D is the vapor diffusivity, and y_1, y_2 the mol fractions of diffusing vapor and inert gas at any point in the film. The velocity of diffusion u_1 (as distinguished from the velocity of molecular thermal agitation) is expressible as the measurable diffusion rate, $N_1/A\theta$ mols/sq.cm/sec., multiplied by the molar volume under the existing partial pressure, $M/\rho y_1$:

$$u_1 = (N_1/A\theta)(M/\rho y_1). \quad (1.13)$$

The other velocity u_2 is given by a similar expression, but for evaporation, as in psychrometry, the second component (air) does not diffuse, and u_2 is zero. Eq. (1.12) becomes

$$N_1/A\theta = -(D\rho/M)(dy_1/dx)/y_2. \quad (1.14)$$

At low partial pressures of vapor, y_1 is small, and y_2 is substantially unity. The mol-fraction gradient dy_1/dx may be replaced by $(y_w - y_b)/B$, and the vapor conductance of the film becomes

$$f_f = (N_1/A\theta)/(y_w - y_b) = (D\rho/M)/B. \quad (1.15)$$

The term $D\rho/M$ may be regarded as a diffusivity expressed in molar units; D is in cm²/sec., that is, cm³/cm²/sec./cm, and $D\rho/M$ is therefore mols/cm²/sec./cm thickness.

Material Transfer by Convection

The Reynolds analogy may be applied to vapor transfer, as was suggested by Royds,[11] though he derived no equation. Consider a particle containing n mols of gas, moving from a point at which the vapor mol-fraction is y_a to a point where it is y_b. The particle initially contains ny_a mols of vapor; moving up to the film boundary and attaining equilibrium with the gas there, the final amount of vapor becomes ny_b. The mols of vapor transferred are

$$N = n(y_b - y_a). \quad (1.16)$$

The momentum loss is $nN_a(u_a - u_b)$, M_a being the average molecular weight in the gas stream, equivalent to M_{air}. With Eq. (1.04), the vapor conductance in the turbulent zone is

$$f_c = (N/A\theta)/(y_b - y_a) = F/M_a(u_a - u_b). \quad (1.17)$$

An equation of this type has been derived by Sherwood.[12] An expression analogous to Eq. (1.07) is obtained by using Eq. (1.06),

$$f_c = Zu_b/BM_a(u_a - u_b) = Zr/BM_a(1-r). \quad (1.18)$$

Material Transfer by Diffusion and Convection

The analog of Eq. (1.11) is secured by combining Eqs. (1.15) and (1.18); adding resistances,

$$1/f_g = 1/f_c + 1/f_f = BM_a(1-r)/rZ + BM_a/D\rho_a. \quad (1.19)$$

Inverting and rearranging,

$$f_g = \frac{(D\rho/M)}{B}\left[\frac{Z/D\rho_a + (1-r)/r}{Z/D\rho_a}\right]. \quad (1.20)^{13}$$

Application to the Psychrometer

The application of the expressions obtained for h_g and f_g to the processes occurring at the wet bulb will result in a new psychrometer theory. An additional equation arises from the adiabaticity of the wet bulb at equilibrium, a balance between incoming sensible heat and outgoing latent heat:

$$Q/A\theta = (N/A\theta)(M_v\lambda). \quad (1.21)$$

To the latent heat λ should properly be added

[9] Prandtl, Phys. Zeits. **11**, 1072 (1910) and Taylor, Brit. Advisory Comm. Aero., Rep. and Mem. **1**, 423 (1916), derived a related convection-conduction equation, not explicit in the film conductance.

[10] Stefan, Wien Ber. **68**, 385 (1873).

[11] Chang, *Thesis*, Mass. Inst. Tech., 1928; Lewis and Chang, Trans. Am. Inst. Chem. Eng. **21**, 127 (1928).

[12] Sherwood, Unpublished Notes, Mass. Inst. Tech., 1924.

[13] Colburn, Ind. Eng. Chem. **22**, 969 (1930) has derived a similar expression, analogous to that of Prandtl.

a small term representing the sensible heat of the vapor, but for practical purposes this correction may be neglected.

From a combination of Eqs. (1.01), (1.11) and (1.20), a general expression for **A** in terms of h_g and f_g results:

$$\mathbf{A}=\frac{y_w-y_a}{t_a-t_w}=\frac{(N/A\theta)/f_g}{(Q/A\theta)/h_g}=\frac{h_g}{f_g(M_v\lambda)}. \quad (1.22)$$

The value of **A** is determined by the theoretical value of h_g/f_g. If this ratio be set equal to h_c/f_c (convectional resistance of controlling importance), the result is

$$\mathbf{A}=h_c/f_c(M_v\lambda)=M_aC/M_v\lambda, \quad (1.23)$$

which is identical with Eq. (1.02) as derived by Gay-Lussac, Ivory, August and Apjohn, without the use of the Reynolds analogy as an intermediate step. Eq. (1.23) results from any theory in which the transfer rates for heat and vapor are the same.

If the principal resistance is assumed to reside in the film, h_f/f_f may be used instead of h_g/f_g, whence, by Eqs. (1.09) and (1.15),

$$\mathbf{A}=(kM_a/D\rho_a)/M_v\lambda\equiv(M_aC/M_v\lambda)(K/D). \quad (1.24)$$

K is the thermal diffusivity, $k/C\rho$. This is similar to the equation obtained by Maxwell, although he employed an additional term to allow for radiative heat transfer. Comparison with the preceding equation indicates that the result of the diffusional theory differs from that of the convectional theory only by the inclusion of the ratio K/D, the ratio of the thermal diffusivity to the vapor diffusivity. Although the mechanisms of heat and material transfer are the same, the rates are not the same (as is true for convective transfer) and the diffusivities must be introduced.

The New Psychrometer Equation

A physically complete equation, neglecting neither convection nor diffusion, may be derived by combining Eqs. (1.11), (1.20) and (1.22):

$$\mathbf{A}=\frac{h_g}{f_g(M_v\lambda)}=\frac{M_aC}{M_v\lambda}\left\{\frac{(1-r)/r+Z/D\rho_a}{(1-r)/r+CZ/k}\right\}. \quad (1.25)$$

The bracketed term contains three criteria: $(1-r)/r$, which determines the resistance to the transfer of both heat and vapor in the turbulent zone; CZ/k, for heat transfer by conduction in the film; and $Z/D\rho$ for vapor transfer by diffusion. Gibson[14] pointed out the important fact that for heat transfer the resistance in the turbulent zone bears a ratio $(1-r)/r : CZ/k$ to the resistance in the film. Although C refers to the stream and Z and k to the film, it is convenient to group these three quantities together in the dimensionless ratio CZ/k; usually it is nearly constant throughout the system. CZ/k may be regarded as the ratio of the kinematic viscosity (momentum diffusivity) to the thermal diffusivity $k/C\rho$. $Z/D\rho$ is similarly the ratio of Z/ρ to the vapor diffusivity D. If $(1-r)/r$ is large relative to CZ/k and $Z/D\rho$, Eq. (1.25) reduces to Eq. (1.23); if $(1-r)/r$ is relatively small, Eq. (1.24) results, since the convectional resistance is then unimportant. The correct value of **A** lies between the limits formed by these two equations, representing the special cases of convection controlling (1.23) and conduction controlling (1.24).

There exists an important special case, for which Eq. (1.25) reduces to the convection-theory result, although convection is not controlling: when $Z/D\rho$ and CZ/k are equal, the bracketed term becomes unity, and Eqs. (1.23), (1.24), and (1.25) are identical. Since Z appears in both criteria, the condition for the identity may be written

$$k/C\rho=K=D, \quad (1.26)$$

the thermal diffusivity being equal to the vapor diffusivity, and the rates of flow of heat and vapor through the film equal. The importance of this special case arises from the fact that Eq. (1.26) is very nearly true for the system water-air at ordinary temperatures. To this fortuitous equality the Maxwell and August equations owe their approximate agreement with the results of atmospheric humidity measurements.

Engineering Notation

In engineering calculations, it is customary to express the moisture content of the air as a

[14] Gibson, *The Mechanical Properties of Fluids*, p. 178, Van Nostrand, New York, 1924.

humidity, H, or (weight of vapor)/(weight of dry air), instead of a partial pressure, p. H is defined by the equation

$$H=(M_v p)/M_a(P-p)\equiv yM_v/M_a, \quad (1.27)$$

$p/(P-p)$ being substantially equal to p/P, or y, at low vapor contents. Instead of the ordinary specific heat, C, it is convenient to use the *humid heat*, s, defined as the total heat capacity associated with unit weight of dry air; when H is small, s is equivalent to C:

$$s=C_{\text{gas}}+C_{\text{vapor}}\equiv C_{\text{gas}}. \quad (1.28)$$

For the evaporation of water into air, Eq. (1.23) is approximately correct, and may be combined with Eqs. (1.01) and (1.27) to give

$$s/\lambda=(H_w-H_a)/(t_a-t_w). \quad (1.29)$$

The importance of this relationship arises from its formal identity with the heat balance for the adiabatic saturation of air, the sensible heat lost by the air being $s(t_a-t_w)$ and the latent heat required for evaporation $\lambda(H_w-H_a)$. The approximate validity of Eq. (1.23) has long been known as an empirical fact, and Eq. (1.29) has been made the basis for the reduction of psychrometric observations with the aid of the Grosvenor-Carrier[15] humidity chart. On this chart, the adiabatic cooling lines, with a slope of $-s/\lambda$, may be used as psychrometric lines, which should have a slope of $-h_g/M_a f_g\lambda$. The error involved in this procedure is slight, for water on the wet bulb at about room temperature; at high temperatures and humidities, or for other liquids, the error may become very great.

The Radiation Correction

In the derivation of Eq. (1.25), it was assumed that all the heat reaching the wet bulb was transferred by convection and conduction. In practice, however, radiant heat must be considered, unless precautions are taken to render it negligible. Instead of h_g, Eq. (1.22) should contain h_g+h_r, where h_r is the conductance for radiant heat; the right-hand side of Eq. (1.25) should therefore be multiplied by the ratio $(h_g+h_r)/h_g$, or $1+h_r/h_g$.

The Stefan-Boltzmann equation is used to find h_r; for small temperature differences, it may be simplified to

$$h_r=c(4T^3)/[1/\epsilon_w+(A_w/A_s)(1/\epsilon_s-1)]. \quad (1.30)$$

This formula applies to two bodies of A_w/A_s area ratio and thermal emissivities ϵ_w and ϵ_s—in this case the wet bulb and the glass tube enclosing it. T is the average temperature, absolute, of the bulb and tube. The emissivity of the glass is about 0.90; for water, the only known determination is that of Siegl,[16] about 0.67, which appears to be much too low. The emissivities of other liquids apparently have never been determined. Consequently, an assumed value of 0.90 will be used for all liquids. A_w/A_s is the same as the ratio of the radii, 7/13; T is roughly 290°K; c is 0.000137 cal./sq.cm/sec./(deg.C/100)^4.

The value of h_g may be estimated with the aid of the empirical equation of Dixon,[17]

$$h_g=54CT^{-1}(u_a\rho_a)^{0.8}/10^6 d^{0.2}. \quad (1.31)$$

The equivalent diameter, d, is the clearance between the wet-bulb surface and the U-tube wall, 0.3 cm. Values of h_g, in calories/sq.cm/sec./deg.C, $\times 10^4$, are given in Table III. The value of h_r is the same for all velocities, 1.132. The radiation correction, h_r/h_g, amounts to about 15 percent, and must not be omitted, as might be done at very high velocities.

Experimental Test of the New Equation

In order to test Eq. (1.25) effectively, the experimental conditions must be chosen carefully so as not to violate any of the assumptions made in the derivation. It is to be emphasized that the derivation applies to a single point on the wet-bulb surface, and therefore may be expected to be valid for the wet bulb as a whole only when conditions at all points are essentially the same. For the data given below, this requirement appears to be satisfied.

The liquids used must have vapor pressures sufficiently low to prevent the drying out of the wet bulb before equilibrium is attained. Their physical properties, particularly vapor pressures

[15] Grosvenor, Trans. Am. Inst. Chem. Eng. **1**, 1 (1908); Carrier, Trans. Am. Soc. Mech. Eng. **33**, 1311 (1911).

[16] Siegl, Wien Ber. **116**, 1203 (1907).

[17] Walker, Lewis and McAdams, *Principles of Chemical Engineering*, p. 149, McGraw-Hill, New York, 1927.

and latent heats, must be accurately known. The range of variation of K/D should be large; unfortunately, D changes but little from substance to substance, and parallels the change in vapor pressure, so that substances having small values of D have vapor pressures too small to be usable for psychrometric purposes.

Care must be taken that the process of evaporation is not interfered with by the condensation of any constituent of the carrier gas. Unless the air used is thoroughly dried, hygroscopic liquids cannot be used; moreover, if the wet-bulb temperature falls below the dew-point of the air, condensation of the moisture will occur. The importance of this factor becomes apparent on inspection of Eq. (1.12); when u_2 is large and negative, u_1 must be smaller than when u_2 is zero, and the final equation should be modified accordingly. Counter-diffusion of water vapor, and condensation of water on the wet bulb, must therefore be avoided.

The Apparatus

The liquids chosen to satisfy these conditions were water, methyl alcohol, propyl alcohol, ethyl propionate, and toluene. The air used was dried by passage through two 500 cc. Allihn gas-washing bottles, containing sulfuric acid, and connected in parallel. Two empty bottles, in parallel, served as entrainment traps. Experiment showed that air passed through this system contained insufficient moisture to affect the weight of a calcium chloride tube; others have also obtained high efficiency with this type of dryer. The dried air was metered by a calibrated orifice flowmeter.

The psychrometer itself was very simple, consisting of a four-inch side-arm U-tube of 13 mm inside diameter, carrying two tenth-degree thermometers. One thermometer was covered with six layers of cotton cloth (unbleached muslin) which served as a wick for holding the liquid. The outside diameter of the wick was 7 mm; it was held in place by a small wire wrapped around the upper end. The dried air (drawn from the laboratory compressed-air line) entered the U-tube through the side arm adjacent to the dry-bulb thermometer, passed through the U-tube to the annular space between the wet-bulb thermometer and the tube wall, and left through the second side arm.

The liquid in use was kept cooled to a temperature near that registered by the wet-bulb thermometer, which was removed from the U-tube from time to time and dipped into the liquid. In this way, drying out of the wick was avoided, especial care being taken that the wick was still wet when the temperature was read. Air was blown past the wet bulb until the temperature remained at a constant value, and, by replenishing the liquid on the wick, could be kept at this temperature for any length of time.

The air velocity was inadvertently allowed to vary, as may be seen from Table III below; however, the variation produced no observable change in the wet-bulb temperature, and, since **A** changes very slowly with velocity, may be disregarded.

Reduction of the Data

The values of **A** (Table I) were found from Eq. (1.01), p_a in all cases being zero, since the air was dry. The vapor pressures were found from data in the I.C.T.,[18] by interpolation on a graph of log p against $1/T$. For the two alcohols, the latent heats (Table II) have been found by extrapolation from the boiling-point to the wet-bulb temperature, by using the Kirchhoff equation,[19]

$$-d\lambda/dt = C_{\text{liquid}} - C_{\text{vapor}} \qquad (1.32)$$

and the I.C.T. latent and specific heat data. For toluene and ethyl propionate, λ was found from the Dieterici equation, discussed by the writer in another paper.[20] Unfortunately, the latent heats are not very accurate, and probably are the greatest source of error in the application of Eq. (1.25).

The term K/D is nearly invariant with temperature, changing by 1 percent in about 18°C; for convenience, it is calculated at 0°C, as consideration of its change with temperature is an unnecessary refinement. The best value of k is that of Weber,[21] 5.686×10^{-5} c.g.s. units. The

[18] Washburn, *International Critical Tables* **3**, 215; **5**, 62, 71, 106, 135, McGraw-Hill, New York, 1927.

[19] Kirchhoff, Ann. d. Physik **103**, 177 (1858).

[20] Arnold, Ind. Eng. Chem. **25**, 659 (1933).

[21] Weber, Ann. d. Physik **54**, 325, 481 (1918).

TABLE I.

	t_a	t_w	t_a-t_w	P	$10^6\mathbf{A}$
Water	25.55	9.55	16.00	770	730
Methyl alcohol	25.45	−3.1	28.55	770	1115
Propyl alcohol	23.55	13.35	10.20	769	1179
Toluene	23.70	11.50	12.20	760.5	1467
Ethyl propionate	24.95	10.85	14.10	769	1512

TABLE II.

	D	K/D	λ	M_v	p_w
Water	0.220	0.83	592	18	9.0
Methyl alcohol	.123	1.49	285	32	24.5
Propyl alcohol	.084	2.17	175	60	9.25
Toluene	.071	2.59	105.6	92	13.62
Ethyl propionate	.068	2.67	91.4	102	16.4

TABLE III.

	u_a m/sec.	h_g	$1+\frac{h_r}{h_g}$	$\frac{\mathbf{A}}{(M_aC/M_v\lambda)}$	ψ
Water	3.74	6.51	1.174	1.115	0.950
Methyl alcohol	3.16	5.70	1.199	1.459	1.216
Propyl alcohol	4.45	7.48	1.151	1.771	1.540
Toluene	4.84	7.46	1.152	2.040	1.770
Ethyl propionate	4.42	8.04	1.141	2.020	1.770

specific heat of air[22] is taken as 0.242; the density of air, 0.00129 g/cc.

Except for water, the diffusivities (D) have been calculated by methods given in a previous paper.[23] For water, the value 0.220 has been used; it is also given by the I.C.T.[18] Winkelmann[24] found 0.216; Brown and Escombe[25] 0.229; the result of LeBlanc and Wuppermann,[26] reduced to 0°, is 0.220; a value by Guglielmo,[27] 0.219.

GRAPHICAL METHOD

For plotting the results of psychrometric measurements, Eq. (1.25) is best rewritten, including the radiation correction, as

$$\psi=\frac{\mathbf{A}/(M_aC/M_v\lambda)}{(1+h_r/h_g)}=\left\{\frac{(1-r)/r+(CZ/k)(K/D)}{(1-r)/r+(CZ/k)}\right\}. \tag{1.33}$$

The quantity ψ is a new psychrometric constant; it is the ratio of **A**, corrected for radiation, to the convection-theory **A**. ψ may be plotted against K/D, since the remaining terms in the bracketed expression are constant for a given carrier gas and velocity. The August equation is represented as a straight line parallel to the axis of K/D, while the Maxwell equation is a 45° line through the origin. Eq. (1.33) gives a third line, lying between those predicted by the Maxwell and August expressions; the three lines intersect at a point determined by Eq. (1.26). (Fig. 1.)

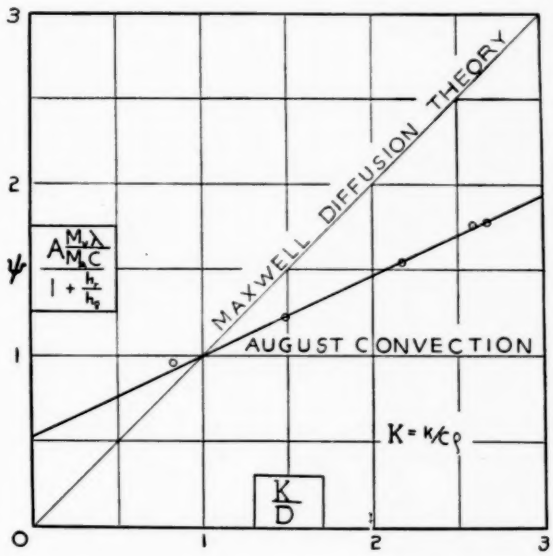

FIG. 1. Comparison of the three theories with observed data.

The points representing the experimental data fall close to a line satisfying the new equation; the agreement is probably enhanced by a partial compensation of errors. For water, the point is close to the intersection of the three lines; hence, any one of the theories gives approximate agreement with experiment, and distinction between complete and incomplete theories can be made only by the use of other liquids or gases.

[22] Carrier, Trans. Am. Soc. Mech. Eng. **44**, 337 (1922); Holborn and Jakob, Zeits. Ver. Deutscher Ing. **58**, 1436 (1913).

[23] Arnold, Ind. Eng. Chem. **22**, 1091 (1930).

[24] Winkelmann, Ann. d. Physik **36**, 93 (1889).

[25] Brown and Escombe, Phil. Trans. Roy. Soc. **B193**, 223 (1900).

[26] LeBlanc and Wuppermann, Zeits. f. physik. Chemie **91**, 143 (1916).

[27] Guglielmo, Atti Accad. Sci. Torino **17**, 54 (1881); **18**, 93 (1882).

The Velocity Ratio

From the intercept on the ψ axis, a value of the criterion $(1-r)/r$ may be calculated. Let b be the value of the intercept; rearranging Eq. (1.33),

$$(1-r)/r=(CZ/k)(b/(1-b)).$$

The value of b read from the graph is 0.52, while CZ/k for air is 0.729; solving, $(1-r)/r$ is 0.787, whence r is 0.56. By Eq. (1.11), the ratio of the convectional resistance to the film resistance is $(1-r)/r : CZ/k$, or 1.08; hence, practically half the resistance to heat transfer is outside the film. For vapor transfer, the ratio varies with D; when $K=D$, it becomes the same as for heat transfer, 1.08.

The graphically-determined value of r may be compared with that found from a theoretical expression given by Prandtl,[28]

$$r=1.75(du_a\rho_a/Z)^{-1/8}=0.55 \qquad (1.35)[29]$$

at a velocity of 4.55 meters/sec. The agreement is excellent; the line on the graph may therefore be regarded as a theoretical line. It is to be remembered that the graphically-determined value of r represents an average taken over the entire wet-bulb surface; but, as conditions do not vary greatly, no appreciable error results from the averaging.

An equation for the film thickness B is derivable from Eq. (1.06) and the empirical relation

$$F=\tfrac{1}{2}f\rho_a u_a^2. \qquad (1.36)$$

The film thickness is

$$B=2Zr/fu_a\rho_a. \qquad (1.37)$$

Since f varies inversely as the fourth root of $du\rho/Z$, and r as the eighth root, B is inversely proportional to the seven-eighths power of the velocity, a fact of considerable importance to psychrometric theory.

Acknowledgment

The writer is indebted to Professor W. K. Lewis, who suggested the problem, for the thought-provoking criticisms offered during the course of the research; and to Dr. T. K. Sherwood for reviewing the manuscript.

[28] Prandtl, Phys. Zeits. **29**, 487 (1928).

[29] Colburn (reference 13) has misquoted this equation, omitting a factor of 2.

The Corrosion of Brass. The Structure of the Corroded Surface

CHARLES W. STILLWELL AND EDWARD S. TURNIPSEED, *Department of Chemistry, University of Illinois*

(Received April 19, 1933)

PRELIMINARY results of an x-ray study of the corroded surface of ϵ-brass indicate that the alloy may corrode in at least two different ways.

(*1*) *Etched in 2N-16N nitric acid.* The ϵ-brass is dissolved as such. The only corrosion layer is a thin layer of copper, probably redeposited by displacement.

(*2*) *Etched in normal sulfuric acid.* After a short etch (4 min.) the layer is copper. As the etching time increases (up to 1 hour) β- and then γ-brass[1] are found in the deposited layer, beneath the copper. The γ-brass is most concentrated next to the unetched ϵ-brass base, the outside layer is copper and between these is β-brass. These phases form a thick (1.0 mm), fairly adherent layer. The following is a possible explanation of the structure: ϵ-brass dissolves as such. Copper is reprecipitated by displacement. As the layer of copper thickens it becomes increasingly difficult for the zinc ions to diffuse through and away from the dissolving surface. As the concentration of zinc ions adjacent to the dissolving surface increases the ratio of the concentrations of copper and zinc ions becomes such that β-brass and later γ-brass may be deposited by displacement.

Acetic acid. Only the zinc is dissolved and the first corrosion layer is γ-brass.

Graf[2] has recently studied the structure of corrosion layers formed when copper-gold alloys are etched. He found that when strong agents were used which could ionize both components, the corrosion layer was pure gold; when weak agents were used the corrosion layer was a solid solution from which part of the copper had been dissolved.

Our preliminary results for corrosion involving change of crystal structure agree in general with Graf's conclusions for corrosion of a solid solution. Strong acids dissolve both metals and the corrosion layer is a redeposited one, first pure copper and after a longer time copper-rich alloys. The weak acid dissolves only zinc and γ-brass is the first corrosion layer.

The complete details and further results of this investigation will be recorded in a paper to be submitted in the near future.

[1] In order of decreasing zinc content the phases of brass are ϵ, γ, β, α.

[2] L. Graf, Metallwirtschaft **11**, 77 (1932).